

# Utilization of Cyclopentylamine as Structure-Directing Agent for the Formation of Fluorinated Gallium Phosphates Exhibiting Extra-Large-Pore Open Frameworks with 16-ring (ULM-16) and 18-ring Channels (MIL-46)

Capucine Sassoze, Jérôme Marrot, Thierry Loiseau,\* and Gérard Férey†

Institut Lavoisier, UMR CNRS 8637, Université de Versailles Saint Quentin en Yvelines, 45 avenue des Etats-Unis, 78035 Versailles Cedex, France

Received September 24, 2001. Revised Manuscript Received November 2, 2001

Two fluorinated gallium phosphates,  $\text{Ga}_4(\text{PO}_4)_4\text{F}_{1.33}(\text{OH})_{0.67} \cdot 1.5\text{NC}_5\text{H}_{12} \cdot 0.5\text{H}_3\text{O} \cdot 0.5\text{H}_2\text{O}$  (ULM-16) and  $\text{Ga}_9(\text{PO}_4)_8\text{F}_{7.3}(\text{OH})_{0.2} \cdot 4\text{NC}_5\text{H}_{12} \cdot 0.5\text{H}_3\text{O} \cdot 3.5\text{H}_2\text{O}$  (MIL-46), have been hydrothermally synthesized by varying the fluorine amount in the presence of cyclopentylamine as structure-directing agent (at 180 °C for 3 days). Their structures were determined by means of single-crystal X-ray diffraction. The first compound (obtained with low fluorine concentration) is isostructural to the gallium phosphate ULM-16 previously prepared with cyclohexylamine. Its three-dimensional framework is built up from the connection by corner sharing of the hexameric units  $\text{Ga}_3(\text{PO}_4)_3\text{F}_2$  together with the tetramer  $\text{Ga}_2(\text{PO}_4)_2$  and consists of channels bound by 16 polyhedra inserting the protonated cyclopentylamine. The second phase (prepared with high fluorine concentration) exhibits a new three-dimensional topology based on the condensation by corner sharing of the identical hexameric building block  $\text{Ga}_3(\text{PO}_4)_3\text{F}_2$  with a pentameric species  $\text{Ga}_5(\text{PO}_4)_5\text{F}_4$ . The resulting network is composed of large 18-ring channels hosting the protonated cyclopentylamine and water molecules. Crystal data are as follows:  $\text{Ga}_4(\text{PO}_4)_4\text{F}_{1.33}(\text{OH})_{0.67} \cdot 1.5\text{NC}_5\text{H}_{12} \cdot 0.5\text{H}_3\text{O} \cdot 0.5\text{H}_2\text{O}$  (ULM-16), orthorhombic, *Pbcn* (no. 60),  $a = 27.316(5)$  Å,  $b = 17.472(3)$  Å,  $c = 10.1970(14)$  Å,  $V = 4866.7(14)$  Å<sup>3</sup> and  $Z = 8$ ;  $\text{Ga}_9(\text{PO}_4)_8\text{F}_{7.3}(\text{OH})_{0.2} \cdot 4\text{NC}_5\text{H}_{12} \cdot 0.5\text{H}_3\text{O} \cdot 3.5\text{H}_2\text{O}$  (MIL-46), orthorhombic, *Pnmm* (no. 58),  $a = 10.2735(2)$  Å,  $b = 18.5962(3)$  Å,  $c = 29.6279(2)$  Å,  $V = 5660.4(2)$  Å<sup>3</sup>,  $Z = 4$ .

## Introduction

Since the discovery of the family of crystalline microporous aluminophosphates in 1982,<sup>1</sup> extensive research has been devoted to the design of novel three-dimensional architectures for their potential applications in the fields of catalysis, ion exchangers, or gas separation. These materials are usually synthesized by the hydrothermal route at low temperature ( $T < 250$  °C, autogenous pressure) by using an organic molecule as structure-directing agent (e.g., amines, quaternary ammoniums). This exploration was extended to the use of many elements of the periodic table, such as B, Ga, Ge, In, Sn, Sb, Be, Mg, or transition metals, and a wide variety of open-framework solids has appeared in the literature.<sup>2</sup> The synthesis of phosphate-based compounds has been considered with a special attention because of the possibility of making extra-large-pore networks. For example, the aluminum phosphate VPI-5<sup>3</sup> containing 18-ring channels and the gallium phosphate cloverite<sup>4</sup> with a three-dimensional 20-ring channel system have been reported. Very recently, the pore size limit was pushed up further and several works described the formation of phases exhibiting channel systems bounded by 24 polyhedra (nickel phosphate VSB-1,<sup>5</sup> zinc phosphate ND-1,<sup>6</sup> zinc phosphonate-carboxylate,<sup>7</sup> gallium phosphate,<sup>8</sup> germanate<sup>9</sup>). In this course, several hydrothermal methods have been tested by adding fluoride anions<sup>10</sup> or nonaqueous solvent<sup>11</sup> (mainly alcohols) in the reaction medium. One successful route was the use of fluorine, which can be incorporated in the gallophosphate matrix and gives rise to the formation of several series of open-framework solids (–CLO,<sup>4</sup> ULM-*n*,<sup>12</sup> MIL-*n*,<sup>13</sup> Mu-*n*,<sup>14</sup> T-GaPO<sup>15</sup>)

phosphate cloverite<sup>4</sup> with a three-dimensional 20-ring channel system have been reported. Very recently, the pore size limit was pushed up further and several works described the formation of phases exhibiting channel systems bounded by 24 polyhedra (nickel phosphate VSB-1,<sup>5</sup> zinc phosphate ND-1,<sup>6</sup> zinc phosphonate-carboxylate,<sup>7</sup> gallium phosphate,<sup>8</sup> germanate<sup>9</sup>). In this course, several hydrothermal methods have been tested by adding fluoride anions<sup>10</sup> or nonaqueous solvent<sup>11</sup> (mainly alcohols) in the reaction medium. One successful route was the use of fluorine, which can be incorporated in the gallophosphate matrix and gives rise to the formation of several series of open-framework solids (–CLO,<sup>4</sup> ULM-*n*,<sup>12</sup> MIL-*n*,<sup>13</sup> Mu-*n*,<sup>14</sup> T-GaPO<sup>15</sup>)

\* To whom correspondence should be addressed. E-mail: loiseau@chimie.uvsq.fr. Phone: (33) 1 39 25 43 73. Fax: (33) 1 39 25 43 58.

† E-mail: ferey@chimie.uvsq.fr.

(1) Wilson, S. T.; Lok, B. M.; Messina, C. A.; Cannan, T. R.; Flanigen, E. M. *J. Am. Chem. Soc.* **1982**, *104*, 1146.

(2) Cheetham, A. K.; Férey, G.; Loiseau, T. *Angew. Chem., Int. Ed.* **1999**, *38*, 3268.

(3) Davis, M. E.; Saldarriaga, C.; Montes, C.; Garces, J. M.; Crowder, C. *Nature* **1988**, *331*, 698.

(4) Estermann, M.; McCusker, L. B.; Baerlocher, C.; Merrouche, A.; Kessler, H. *Nature* **1991**, *352*, 320.

(5) Guillou, N.; Gao, Q.; Nogues, M.; Morris, R. E.; Hervieu, M.; Férey, G.; Cheetham, A. K. *C. R. Acad. Sci., Ser. C* **1999**, *2*, 387.

(6) Yang, G.-Yu.; Sevov, S. C. *J. Am. Chem. Soc.* **1999**, *121*, 8389.

(7) Zhu, J.; Bu, X.; Feng, P.; Stucky, G. D. *J. Am. Chem. Soc.* **2000**, *122*, 11563.

(8) Lin, C.-H.; Wang, S.-L.; Lii, K.-H. *J. Am. Chem. Soc.* **2001**, *123*, 4649.

(9) Zhou, Y.; Zhu, H.; Chen, Z.; Chen, M.; Xu, Y.; Zhang, H.; Zhao, D. *Angew. Chem., Int. Ed.* **2001**, *40*, 2166.

(10) Kessler, H. *Stud. Surf. Sci. Catal.* **1989**, *52*, 17.

(11) Morris, R. E.; Weigel, S. J. *Chem. Soc. Rev.* **1997**, *26*, 309.

(12) Férey, G. *J. Fluorine Chem.* **1995**, *72*, 187.

(13) Férey, G. *C. R. Acad. Sci., Ser. C* **1998**, *1*, 1.

(14) Reinert, P.; Marler, B.; Patarin, J. *Chem. Commun.* **1998**, 1769.

displaying new topologies. This family exhibits a wide diversity of pore systems with channels delimited by 12 rings (TREN–GaPO<sup>15</sup> and GaPO-4-DMAP<sup>16</sup>), 14 rings (DYPIR–GaPO<sup>17</sup>), 16 rings (ULM-5<sup>18</sup> and ULM-16<sup>19</sup>), 18 rings (MIL-31<sup>20</sup>), and 20 rings (–CLO<sup>4</sup> and [N<sub>2</sub>C<sub>4</sub>H<sub>14</sub>]<sub>2</sub>–[Ga<sub>4</sub>(HPO<sub>4</sub>)(PO<sub>4</sub>)<sub>3</sub>(OH,F)<sub>3</sub>·5H<sub>2</sub>O<sup>21</sup>). Besides fluorine, the organic molecule plays a central role for the production of the large-pore solids. For example, the use of variable length of the hydrocarbon chain in the  $\alpha,\omega$ -alkyldiamines showed that the pore size increases with the carbon number. The fluorinated gallium phosphate ULM-5<sup>12</sup> (16-ring channels) is prepared with C<sub>6</sub>, C<sub>7</sub>, and C<sub>8</sub> diamines, whereas MIL-31<sup>20</sup> (18-ring channels) is obtained with C<sub>9</sub> and C<sub>10</sub> diamines.

In our continuing research on the gallium system, we studied the influence of the size of cyclic monoamines on the formation of open frameworks. A previous result reported the crystallization of the large-pore gallium phosphate ULM-16<sup>19</sup> templated with cyclohexylamine. Here, we describe the structure-directing effect of the cyclopentylamine molecule. Depending on the initial fluorine concentration, two distinct phases have been isolated. Ga<sub>4</sub>(PO<sub>4</sub>)<sub>4</sub>F<sub>1.33</sub>(OH)<sub>0.67</sub>·1.5NC<sub>5</sub>H<sub>12</sub>·0.5H<sub>3</sub>O·0.5H<sub>2</sub>O is isostructural with the ULM-16<sup>19</sup> type, and a novel structure Ga<sub>9</sub>(PO<sub>4</sub>)<sub>8</sub>F<sub>7.3</sub>(OH)<sub>0.2</sub>·4NC<sub>5</sub>H<sub>12</sub>·0.5H<sub>3</sub>O·3.5H<sub>2</sub>O named MIL-46 is obtained for higher fluorine content. The three-dimensional framework of MIL-46 contains 18-ring tunnels in which the cyclopentylamine molecules are encapsulated. The hydrothermal synthesis and structural characterization of both compounds are presented in this work.

## Experimental Section

**Synthesis.** Both compounds were prepared under mild hydrothermal conditions using a Teflon-lined 23 cm<sup>3</sup> Parr steel autoclave. The starting chemicals include gallium oxohydroxide (GaOOH, prepared from the reaction of gallium metal with water at 200 °C for 3 days), phosphoric acid (H<sub>3</sub>PO<sub>4</sub>, 85%, Prolabo), hydrofluoric acid (HF, 48%, Prolabo), cyclopentylamine (NC<sub>5</sub>H<sub>11</sub>, 99%, Aldrich), and desionized water.

(a) *ULM-16.* ULM-16 was typically synthesized by mixing GaOOH, H<sub>3</sub>PO<sub>4</sub>, HF, cyclopentylamine, and H<sub>2</sub>O with the molar ratio of 1 (0.713 g):1 (0.4 mL):0.5 (0.144 mL):0.6 (0.354 mL):40 (5 mL). The reactants were placed in the Parr bomb and heated at 180 °C for 3 days. The starting pH was 3 and then 2 after the reaction. The yield of the reaction, based on gallium, was about 20%, but unreacted GaOOH (40%) is still present together with the dense GaPO<sub>4</sub> quartz-type (40%). This yield value is higher compared to that reported in the preparation of ULM-16 obtained with cyclohexylamine (<10%).<sup>22</sup> Some crystals with a specific shape corresponding to the ULM-16 phase have been picked up from the bulk solid for the thermogravimetric (TG) and chemical analysis characterizations.

(15) Weigel, S. J.; Weston, S. C.; Cheetham, A. K.; Stucky, G. D. *Chem. Mater.* **1997**, *9*, 1293.

(16) Bonhomme, F.; Thoma, S. G.; Rodriguez, M. A.; Nenoff, T. M. *Chem. Mater.* **2001**, *13*, 2112.

(17) Weigel, S. J.; Morris, R. E.; Stucky, G. D.; Cheetham, A. K. *J. Mater. Chem.* **1998**, *8*, 1607.

(18) Loiseau, T.; Férey, G. *J. Solid State Chem.* **1994**, *111*, 403.

(19) Loiseau, T.; Férey, G. *J. Mater. Chem.* **1996**, *6*, 1073.

(20) Sassoey, C.; Loiseau, T.; Taulelle, F.; Férey, G. *Chem. Commun.* **2000**, 943.

(21) Chippindale, A. M.; Peacock, K. J.; Cowley, A. R. *J. Solid State Chem.* **1999**, *145*, 379. Walton, R. I.; Millange, F.; Loiseau, T.; O'Hare, D.; Férey, G. *Angew. Chem., Int. Ed.* **2000**, *39*, 4552.

(22) Loiseau, T.; Férey, G. *Mater. Res. Soc. Symp. Proc.* **1996**, *431*, 27.

**Table 1. Crystal Data and Structure Refinement Parameters for the Phases ULM-16 and MIL-46**

	ULM-16	MIL-46
formula	Ga <sub>4</sub> P <sub>4</sub> O <sub>17.67</sub> F <sub>1.33</sub> C <sub>7.5</sub> ·N <sub>1.5</sub> H <sub>20.5</sub>	Ga <sub>4.5</sub> P <sub>4</sub> O <sub>18.1</sub> F <sub>3.65</sub> N <sub>2</sub> ·C <sub>10</sub> H <sub>28.35</sub>
fw (g mol <sup>-1</sup> )	842.29	972.95
T (K)	296(2)	296(2)
wavelength (Å)	0.71073	
cryst sys	orthorhombic	
space group	<i>Pbcn</i> (No. 60)	<i>Pnnm</i> (No. 58)
unit cell dimensions (Å)	<i>a</i> = 27.316(5) <i>b</i> = 17.472(3) <i>c</i> = 10.1970(14)	<i>a</i> = 10.2735(2) <i>b</i> = 18.5962(3) <i>c</i> = 29.6279(2)
<i>V</i> (Å <sup>3</sup> )	4866.7(14)	5660.4(2)
<i>Z</i>	8	8
calcd density	2.300	2.288
abs coeff (mm <sup>-1</sup> )	4.735	4.561
<i>F</i> (000)	3124	3610
cryst size (mm <sup>3</sup> )	0.16 × 0.08 × 0.01	0.5 × 0.02 × 0.01
$\theta$ range for data collection (deg)	1.38–29.84	1.29–23.30
limiting indices	–34 ≤ <i>h</i> ≤ 37 –24 ≤ <i>k</i> ≤ 13 –14 ≤ <i>l</i> ≤ 13	–9 ≤ <i>h</i> ≤ 11 –20 ≤ <i>k</i> ≤ 19 –32 ≤ <i>l</i> ≤ 32
reflns collected	26 238	24 740
independent reflns	6481 [ <i>R</i> (int) = 0.0691]	4163 [ <i>R</i> (int) = 0.1330]
refinement method	full-matrix least-squares on <i>F</i> <sup>2</sup>	
data/restraints/params	6481/5/317	4163/18/392
GOF on <i>F</i> <sup>2</sup>	0.812	0.882
final <i>R</i> indices [ <i>I</i> > 2 $\sigma$ ( <i>I</i> )]	<i>R</i> 1 = 0.0523 <i>wR</i> 2 = 0.1283	<i>R</i> 1 = 0.0655 <i>wR</i> 2 = 0.1547
<i>R</i> indices (all data)	<i>R</i> 1 = 0.0904 <i>wR</i> 2 = 0.1610	<i>R</i> 1 = 0.1099 <i>wR</i> 2 = 0.1864
extinction coeff	0.00037(6)	0.00015(5)
largest diff. peak and hole (e Å <sup>-3</sup> )	2.485 and –1.092	1.204 and –1.613

(b) *MIL-46.* MIL-46 crystallizes for a higher fluorine concentration. It was prepared by mixing GaOOH, H<sub>3</sub>PO<sub>4</sub>, HF, cyclopentylamine, and H<sub>2</sub>O with the molar ratio of 1 (0.713 g):1 (0.4 mL):1.5 (0.433 mL):1 (0.59 mL):40 (5 mL). The reactants were placed in the Parr bomb and heated at 180 °C for 3 days. The pH was 2 before reaction and then rose to 3 at the end. The product is obtained as a pure phase with a yield of 85% based on gallium.

The resulting white powders were filtered off, washed with desionized water, and dried at room temperature. Both compounds are characterized by elongated needle-shaped crystals.

**Crystal Structure Determinations.** A transparent needle-shaped single crystal of each compound was carefully selected under a polarizing optical microscope and was mounted with Araldite on a glass fiber. Room-temperature intensity data collection was performed on a Siemens SMART three-circle diffractometer equipped with a CCD bidimensional detector. The crystal-to-detector distance was 45 mm allowing for data collection up to 60° (2 $\theta$ ). Slightly more than one hemisphere of data was recorded. The frames were collected with a scan width of 0.3° in  $\omega$  and an exposure time of 30 s per frame. Crystal data and details of the data collection are given in Table 1. An empirical absorption correction was applied using the SADABS program<sup>23</sup> based on the method of Blessing.<sup>24</sup>

The structure of the ULM-16 phase was refined in the space group *Pbcn* by using the atomic coordinates of the mineral network (Ga, P, O, F) coming from the structural determination of ULM-16<sup>19</sup> obtained with cyclohexylamine (orthorhombic system, *a* = 27.329(4) Å, *b* = 17.377(2) Å, *c* = 10.214(5) Å). The refinement was performed with the SHELXTL<sup>25</sup> package. The water and cyclopentylamine molecules were found from the

(23) Sheldrick, G. M. *SADABS, a program for the Siemens Area Detector ABSorption correction*; University of Göttingen: Göttingen, Germany, 1995.

(24) Blessing, R. *Acta Crystallogr.* **1995**, *A51*, 33.

examination of successive difference Fourier maps. One of the two crystallographically inequivalent amines, around the special position 4c, is located on two symmetrical positions and was refined with geometric constraints. The hydrogen atoms were not included in the refinements. The final reliability factors, with anisotropic temperature parameters, converge to  $R1 = 0.0523$  and  $wR2 = 0.1283$  (for 6481 reflections  $I > 2\sigma(I)$ ) with 317 parameters.

The structure of MIL-46 was solved in the space group  $Pnmm$  by using the direct methods of the SHELXTL<sup>25</sup> package. The positions of gallium and phosphorus atoms were first found, and the remaining atoms (F, O, N, C) were placed from successive Fourier map analyses. The fluorine atoms were located from considerations of the temperature factors and bond-valence calculations. Three sites (noted F1, F2, and F3) are in the general position 8h. The sites F4 and F5 are in the special positions 4g and 2c, respectively. F5 connects two gallium atoms together, and F4 is found in a terminal Ga–F bonding. Three crystallographically inequivalent amines are found within the larger channels and were refined with geometric constraints. The nitrogen N3 was refined with a 50% occupancy factor because of the symmetry restraints. Two water molecules (Ow1 and Ow2) were then placed within the pores. At this stage, the difference Fourier map revealed two residues ( $\sim 4e^- \text{ \AA}^3$ ) close to each other ( $\sim 1.80 \text{ \AA}$ ). These Fourier peaks were attributed to water molecules (Ow3 and Ow4) and refined with a 50% occupancy factor. Some abnormally short distances are observed between the nitrogen N3 and the Ow3 and Ow4 water molecules ( $\sim 1.83 \text{ \AA}$ ) because of symmetry operations. But these interactions can be minimized by considering a scheme in which the shortest distances are excluded in correlation with the 50% occupancy of these atoms. For a given occupancy of the nitrogen N3, one may consider that the closest atom, Ow4, is located on the opposite site, and the N3–Ow4 distance becomes 3.32 Å. The same argument can be used for the positions of Ow3 correlated to those of Ow4. However, the final reliability factor is rather high and prevents accurate placement of the different configurations occupied by the amine N3 and the water molecules Ow3 and Ow4. The amines were refined with geometric constraints. The reliability factors converge to  $R1 = 0.0655$  and  $wR2 = 0.1547$  (for 4163 reflections  $I > 2\sigma(I)$ ) with 392 parameters.

The resulting atomic coordinates including isotropic temperature parameters of ULM-16 and MIL-46 are shown in the Tables 2 and 3, respectively. A selection of bond distances and angles may be obtained on request to the authors.

**Characterizations.** The fluorine amount of the samples was obtained by a potentiometric method with a fluoride ion selective electrode. For ULM-16, the chemical analysis gives 3.05% and corresponds to 1.33 F for 4  $\text{GaPO}_4$  units. Two crystallographic sites (noted F1 and F2) are compatible with the presence of fluorine (or charge  $-1$  from the bond-valence calculations<sup>26</sup>), and this results that 0.67 OH are present. These two positions are statistically occupied by fluorine and hydroxyl group with the 2/1 ratio.

As assumed from the synthesis conditions, the fluorine content is much higher for the phase MIL-46. The chemical analysis gives 7.19% and corresponds to 7.3 F for 1  $\text{Ga}_9(\text{PO}_4)_8$  unit. The five possible sites of charge  $-1$  (from the bond-valence calculations<sup>26</sup>) assigned to fluorine (F1, F2, F3, F4, and F5) have a multiplicity of 7.5 (for the  $\text{Ga}_9(\text{PO}_4)_8$  unit). This indicates that these sites are mainly occupied by fluorine. With respect to bond-valence considerations and uncertainties from the fluorine chemical analysis, a small amount of hydroxyl groups (0.2 OH) might be statistically present on these positions. The <sup>19</sup>F MAS NMR spectrum showed two groups of unresolved broad resonance peaks located at  $-90$  and  $-110$  ppm. This result is in agreement with the occurrence of Ga–F bonding, but the poor resolution observed for this spectrum prevented us from assigning the different crystallographic sites

**Table 2. Atomic Coordinates ( $\times 10^4$ ) for Non-Hydrogen Atoms (with Standard Deviations in the Least Significant Digits in Parentheses) and Equivalent Isotropic Atomic Displacement Parameters ( $\text{\AA}^2 \times 10^3$ ) for ULM-16 ( $U_{\text{eq}}$  Is Defined as the One-Third of the Trace of the Orthogonalized  $U_{ij}$  Tensor)**

atom	x	y	z	$U_{\text{eq}}$	Wyckoff
Ga(1)	2203(1)	2392(1)	884(1)	13(1)	8d
Ga(2)	3441(1)	1793(1)	1105(1)	15(1)	8d
Ga(3)	540(1)	4235(1)	-975(1)	18(1)	8d
Ga(4)	2415(1)	4127(1)	-740(1)	18(1)	8d
P(1)	1416(1)	3198(1)	-960(2)	14(1)	8d
P(2)	2552(1)	657(1)	1105(2)	15(1)	8d
P(3)	-596(1)	4258(1)	-948(2)	16(1)	8d
P(4)	3040(1)	2734(1)	-1140(2)	15(1)	8d
F(1)	2839(1)	2302(2)	1793(4)	20(1)	8d
F(2)	2325(2)	3524(2)	937(4)	26(1)	8d
O(1)	2173(2)	1281(2)	871(4)	17(1)	8d
O(2)	2568(2)	2339(2)	-739(4)	16(1)	8d
O(3)	4041(2)	1321(3)	479(5)	26(1)	8d
O(4)	1765(2)	3879(3)	-1121(5)	21(1)	8d
O(5)	-613(2)	4958(3)	-83(6)	44(2)	8d
O(6)	937(2)	3503(3)	-304(5)	23(1)	8d
O(7)	2992(2)	3606(3)	-1016(5)	20(1)	8d
O(8)	2571(2)	5008(3)	160(5)	22(1)	8d
O(9)	1828(2)	2490(3)	2455(4)	19(1)	8d
O(10)	2465(2)	4652(3)	-2478(4)	22(1)	8d
O(11)	1607(2)	2550(3)	-127(4)	19(1)	8d
O(12)	3473(2)	2479(3)	-272(4)	18(1)	8d
O(13)	3082(2)	915(2)	785(5)	19(1)	8d
O(14)	3731(2)	2083(3)	2669(4)	22(1)	8d
O(15)	697(2)	4530(3)	-2640(5)	27(1)	8d
O(16)	-85(2)	3884(3)	-888(6)	33(1)	8d
OW	1598(4)	5720(5)	-2219(10)	78(3)	8d
N(1)	3059(3)	3872(4)	2965(8)	40(2)	8d
C(1)	3557(5)	4130(14)	2798(17)	123(8)	8d
C(2)	3751(6)	4310(14)	1571(13)	129(9)	8d
C(3)	4275(7)	4519(19)	1891(22)	190(14)	8d
C(4)	4309(8)	4540(21)	3345(24)	206(16)	8d
C(5)	3840(6)	4332(14)	3899(15)	130(9)	8d
N(2)	856(6)	6868(9)	-2415(15)	42(3)	8d
C(6)	0	7087(28)	-2500	206(19)	4c
C(7)	442(14)	7604(21)	-2262(44)	130(14)	8d
C(8)	11(21)	8349(27)	-3121(50)	170(21)	8d
C(9)	404(21)	7931(35)	-3558(51)	187(23)	8d

occupied by fluorine. TGA measurements were carried out on a TA-Instrument type 2050 thermoanalyzer ( $\text{O}_2$  gas flow; heating rate,  $2 \text{ }^\circ\text{C}/\text{min}$  between  $25 \text{ }^\circ\text{C}$  and  $1050 \text{ }^\circ\text{C}$ ).

## Results

**Structure of ULM-16,  $\text{Ga}_4(\text{PO}_4)_4\text{F}_{1.33}(\text{OH})_{0.67} \cdot 1.5\text{NC}_5\text{H}_{12} \cdot 0.5\text{H}_3\text{O} \cdot 0.5\text{H}_2\text{O}$ .** The compound exhibits a three-dimensional framework incorporating water and cyclopentylamine molecules within the pores. The inorganic network is similar to that reported previously with cyclohexylamine.<sup>19</sup> It is built up from a rectangular-shaped hexameric unit consisting of three  $\text{PO}_4$  phosphate groups connected to two  $\text{GaO}_4(\text{F},\text{OH})$  trigonal bipyramids and one  $\text{GaO}_4(\text{F},\text{OH})_2$  octahedron (Figure 1a). The octahedral entity located at the center of this hexamer is linked to the trigonal bipyramids via a fluorine/hydroxyl group and the three phosphate groups. This  $\text{Ga}_3\text{P}_3$  unit has been already encountered in many fluorinated gallium phosphates (ULM-8,<sup>27</sup> DAO-GA-PO,<sup>28</sup> MIL-30,<sup>29</sup> ULM-3,<sup>12</sup> ULM-4,<sup>12</sup> TREN-GaPO,<sup>15</sup>

(27) Serpaggi, F.; Loiseau, T.; Riou, D.; Hosseini, M. W.; Férey, G. *Eur. J. Solid State Inorg. Chem.* **1994**, *31*, 595.

(28) Weigel, S. J. Ph.D. Thesis Dissertation, University of Santa Barbara, Santa Barbara, California, 1996.

(29) Paulet, C.; Loiseau, T.; Férey, G. *J. Mater. Chem.* **2000**, *10*, 1225.

(25) Sheldrick, G. M. *SHELXTL, Software Package for the Crystal Structure Determination*, version 5.03; University of Göttingen: Göttingen, Germany, 1994.

(26) Brese, N.; O'Keefe, M. *Acta Crystallogr. B* **1991**, *47*, 192.



**Table 3. Atomic Coordinates ( $\times 10^4$ ) for Non-Hydrogen Atoms (with Standard Deviations in the Least Significant Digits in Parentheses) and Equivalent Isotropic Atomic Displacement Parameters ( $\text{\AA}^2 \times 10^3$ ) for MIL-46 ( $U_{\text{eq}}$  Is Defined as the One-Third of the Trace of the Orthogonalized  $U_{ij}$  Tensor)**

atom	<i>x</i>	<i>y</i>	<i>z</i>	$U_{\text{eq}}$	Wyckoff
Ga(1)	1415(1)	965(1)	2418(1)	12(1)	8h
Ga(2)	1629(1)	2871(1)	2666(1)	11(1)	8h
Ga(3)	3395(1)	3363(1)	1679(1)	16(1)	8h
Ga(4)	11896(2)	4955(1)	0	25(1)	4g
Ga(5)	8625(2)	4209(1)	1057(1)	58(1)	8h
P(1)	1515(3)	-759(2)	2393(1)	12(1)	8h
P(2)	6488(3)	3380(2)	1593(1)	14(1)	8h
P(3)	3671(3)	1931(2)	2134(1)	12(1)	8h
P(4)	8418(3)	5865(2)	952(1)	22(1)	8h
F(1)	8188(11)	4267(6)	443(4)	75(4)	8h
F(2)	758(6)	2012(3)	2442(2)	16(2)	8h
F(3)	1603(7)	3215(4)	2011(2)	24(2)	8h
F(4)	13725(21)	4993(11)	0	110(7)	4g
F(5)	10000	5000	0	63(6)	2c
O(1)	7463(8)	3530(4)	1210(3)	20(2)	8h
O(2)	8119(12)	5772(5)	453(3)	44(3)	8h
O(3)	3638(8)	2383(4)	1699(3)	18(2)	8h
O(4)	3246(7)	2384(4)	2537(3)	13(2)	8h
O(5)	44(7)	3370(4)	2778(3)	14(2)	8h
O(6)	5123(8)	3522(5)	1397(3)	21(2)	8h
O(7)	7441(9)	6382(5)	1155(3)	28(2)	8h
O(8)	1264(8)	-944(4)	2894(3)	18(2)	8h
O(9)	2064(8)	-3(4)	2366(3)	20(2)	8h
O(10)	8363(9)	5142(5)	1208(3)	28(2)	8h
O(11)	2771(8)	1279(4)	2055(3)	16(2)	8h
O(12)	1685(8)	2402(4)	3262(3)	16(2)	8h
O(13)	2544(7)	3734(4)	2846(3)	13(2)	8h
O(14)	1783(8)	1071(4)	3030(3)	18(2)	8h
O(15)	-194(7)	798(4)	2144(3)	17(2)	8h
O(16)	9780(9)	6190(5)	1004(4)	44(3)	8h
OW1	4855(16)	1807(9)	5000	52(4)	4g
OW2	9503(14)	4351(9)	1917(7)	136(9)	8h
OW3	0	0	3961(9)	35(7)	4e
OW4	15000	5000	424(8)	36(7)	4e
N(1)	-455(11)	2245(6)	1586(4)	29(3)	8h
C(1)	-306(14)	2052(11)	1097(5)	59(6)	8h
C(2)	-1349(20)	1588(14)	925(9)	112(11)	8h
C(3)	-662(30)	961(21)	756(20)	285(36)	8h
C(4)	741(28)	1103(21)	720(19)	257(31)	8h
C(5)	990(18)	1729(13)	993(7)	81(7)	8h
N(2)	5000	0	1978(5)	48(5)	4f
C(6)	5000	0	1512(8)	130(18)	4f
C(8)	3971(35)	-67(31)	1235(7)	228(26)	8h
C(7)	4383(42)	-142(35)	780(9)	265(30)	8h
N(3)	10022(25)	1166(18)	4554(9)	52(8)	8h
C(9)	9995	1843	4758	267(32)	8h
C(11)	6166(42)	7496(45)	0	271(41)	4g
C(10)	3	2711	4672	276(33)	8h

ULM-5,<sup>18</sup> MIL-31<sup>20</sup>), and it is linked together to generate a plane along (100). In this layer, two adjacent hexameric species have different orientations. The sheets are connected to each other through a tetrameric unit  $\text{Ga}_2(\text{PO}_4)_2$  (Figure 1b) forming infinite double crankshaft chains along [001] and composed of  $\text{PO}_4$  tetrahedra alternating with  $\text{GaO}_4$  tetrahedra (Figure 1c). This type of tetrahedra-based double chain was noted *cc* in the nomenclature given by Smith for the description of silicates.<sup>30</sup> The  $\text{PO}_4$ ,  $\text{GaO}_4$ ,  $\text{GaO}_4(\text{F},\text{OH})$ , and  $\text{GaO}_4(\text{F},\text{OH})_2$  polyhedra share all of their corners with each other with strict respect of the Ga–O–P bonding. Only fluorine/hydroxyl groups are found in bridging positions between the gallium atoms. This connection mode induces a 3D open framework delimiting 16-ring channels running along [001] together with

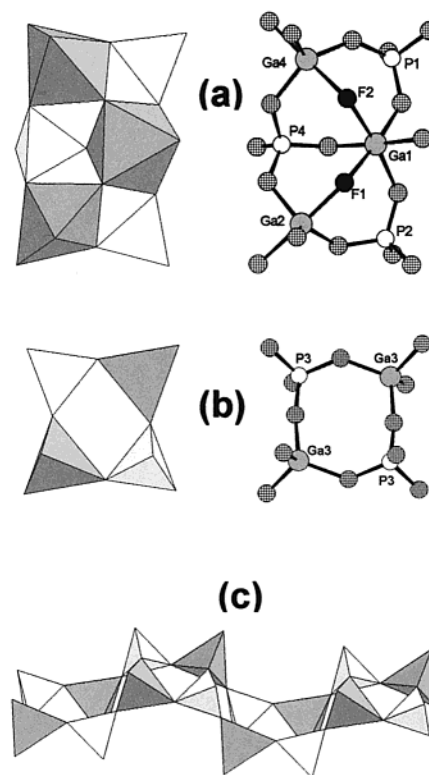


**Figure 1.** Polyhedral and ball-and-stick representations of the building blocks in ULM-16: (a) hexameric unit  $\text{Ga}_3(\text{PO}_4)_3-(\text{F},\text{OH})_2$ ; (b) tetrameric unit  $\text{Ga}_2(\text{PO}_4)_2$ , unlabeled hatched circles = oxygen atoms; (c) mode of connection of the tetrameric units leading to the formation of the infinite double crankshaft chain, *cc*, running the *c* axis.

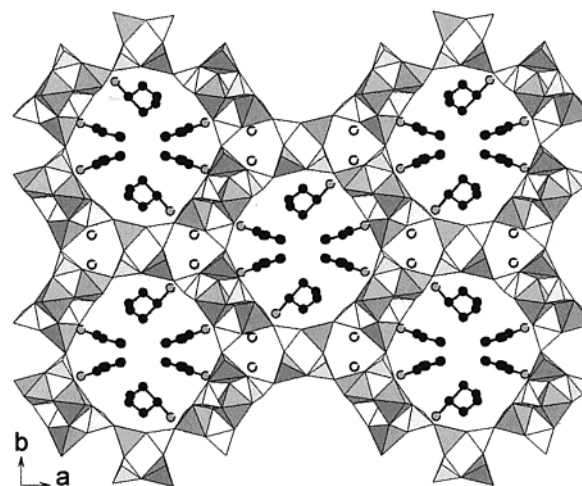


**Figure 2.** View of the structure of ULM-16 showing the 16-ring channels encapsulating the cyclopentylamine molecules along the *c* axis: white polyhedra,  $\text{PO}_4$ ; gray polyhedra,  $\text{GaO}_4$ ; open circles, water molecules; gray circles, nitrogen atoms; black circles, carbon atoms.

6-ring ones (Figure 2). The calculated free diameter of the 16-ring pores is  $10.5 \text{ \AA} \times 11 \text{ \AA}$  (based on an oxygen ionic radius of  $1.35 \text{ \AA}$ ).

The P–O and Ga–O distances are as expected for the different observed geometries (P–O<sub>tetrahedral</sub> in the range of  $1.495\text{--}1.562 \text{ \AA}$ , Ga–O<sub>tetrahedral</sub> in the range of  $1.787\text{--}1.825 \text{ \AA}$ , Ga–O<sub>bipyramidal</sub> in the range of  $1.842\text{--}1.869 \text{ \AA}$  (equatorial plane), and Ga–O<sub>octahedral</sub> in the range of  $1.910\text{--}1.946 \text{ \AA}$ ). Only the Ga–(F,OH) distances are

(30) Smith, J. V. *Chem. Rev.* **1988**, *88*, 149.

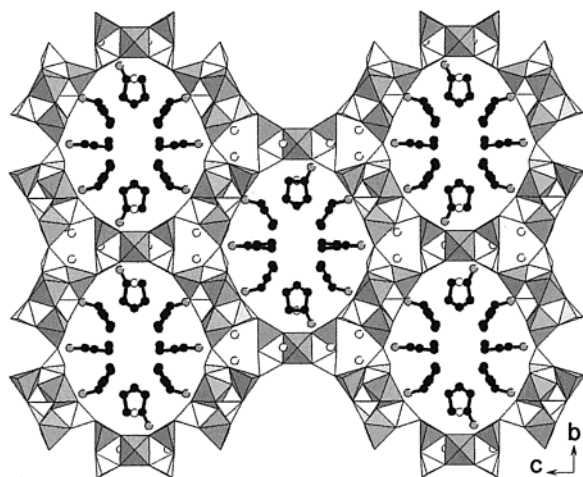


**Figure 3.** View of the structure of MIL-46 showing the 18-ring channels hosting the cyclopentylamine and water molecules along the *a* axis: white polyhedra, phosphorus; gray polyhedra, gallium; open circles, water molecules; gray circles, nitrogen atoms; black circles, carbon atoms.

slightly longer because of the preferential interaction with the monoamines ( $\text{Ga}-\text{F} = 1.977\text{--}2.024 \text{ \AA}$ ).

The water molecules are trapped within the 6-ring channels, whereas the organic amines are located in the 16-ring ones. The cyclopentylamines are protonated, and each ammonium group points toward the anions of the mineral framework. This situation is identical to that observed in the gallium phosphate ULM-16 prepared with cyclohexylamine.<sup>19</sup> In both compounds, the number and the positions of the ammonium groups are identical. Strong hydrogen bondings are observed between the nitrogen atoms and the anions F and O (mainly those bridging the gallium atoms). It results that the cyclopentane groups point toward the center of the largest channels. On a smaller scale, this disposition resembles the interaction of surfactant molecules within the channels of mesoporous compounds<sup>31,32</sup> (MCM-41 series). In this class of materials, the templating agent consists of long alkyl chains with a hydrophilic charged head (e.g., quaternary ammoniums, phosphates) and a hydrophobic tail (e.g., methyl). In solution, the electrostatic energy minimization induces the formation of spheric, layered, or tubular assemblies (micelles), which will play a templating role. The hydrophilic heads of the surfactant, usually located at the surface of the micelles, interact with the silicates walls, and the hydrophobic tails converge toward the center of pores where van der Waals interactions occur. A similar behavior was discussed in the extra-large-pore zincophosphate ND-1<sup>6</sup> showing the cyclohexane groups of the structure-directing agent (1,2-diaminocyclohexane) pointing toward the center of the 24-ring tunnels.

**Structure of MIL-46,  $\text{Ga}_9(\text{PO}_4)_8\text{F}_{7.3}(\text{OH})_{0.2}\cdot 4\text{N-C}_5\text{H}_{12}\cdot 0.5\text{H}_2\text{O}\cdot 3.5\text{H}_2\text{O}$ .** The inorganic framework of MIL-46 is reminiscent of that of MIL-31<sup>20</sup> because of the occurrence of the large 18-ring and 6-ring channels (Figure 3). These tunnels are running along [100] and

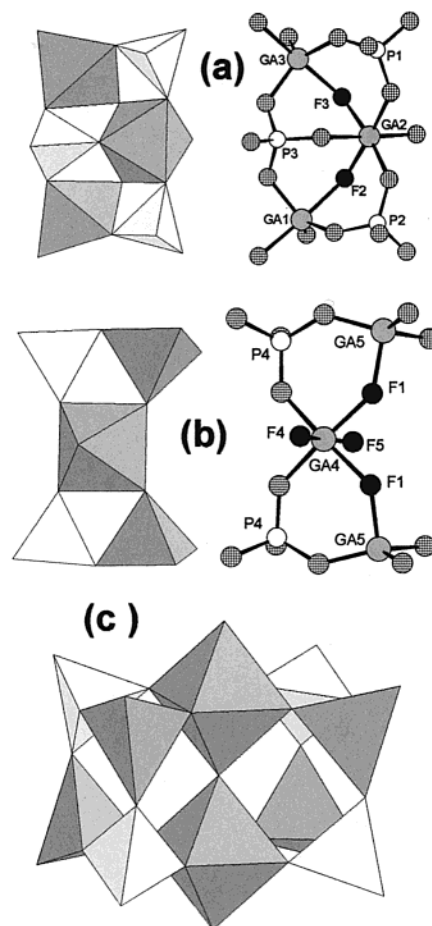


**Figure 4.** Polyhedral and ball-and-stick representations of the building blocks in MIL-46: (a) hexameric unit  $\text{Ga}_3(\text{PO}_4)_3\text{F}_2$ ; (b) pentameric unit  $\text{Ga}_3(\text{PO}_4)_2\text{F}_4$  in which the fluorine F4 is terminal; unlabeled hatched circles, oxygen atoms; (c) mode of the  $\text{Ga}-\text{O}-\text{P}$  connection by corner sharing of two pentameric species along the *a* axis. The fluorine F5 is in bridging position between the octahedrally coordinated gallium, Ga4.

are delimited by  $\text{Ga}_3\text{P}_3$  hexameric units connected to a  $\text{Ga}_3\text{P}_2$  pentameric unit. The hexameric building block is identical to that previously described in ULM-16 in this work and consists of three tetrahedral phosphate groups,  $\text{PO}_4$ , two trigonal bipyramids,  $\text{GaO}_4\text{F}$ , and one octahedron,  $\text{GaO}_4\text{F}_2$  (Figure 4a). Its edge-sharing connection mode is similar and generates the same type of plane along (110). The  $\text{PO}_4$  tetrahedra are regular with  $\text{P}-\text{O}$  distances ranging from 1.514 to 1.546  $\text{\AA}$ . The gallium polyhedra are distorted due to the longer  $\text{Ga}-\text{F}$  distances ( $\sim 2.0 \text{ \AA}$ ). The  $\text{Ga}-\text{O}$  distances are in the range of 1.837–1.868  $\text{\AA}$  for the trigonal bipyramid and 1.903–1.969  $\text{\AA}$  for the octahedron.

The sheets of hexameric units are connected through another type of building block consisting of two phosphate groups and three gallium atoms (Figure 4b). The central gallium (Ga4) atom is octahedrally coordinated with four fluorine atoms and two oxygen atoms ( $\text{GaO}_2\text{F}_4$ ). It is linked to the two phosphate groups by the oxygen atoms and to two other gallium atoms by the fluorine atoms. These four anions are located in one square plane of the octahedron, the fluorine atoms being placed in cis position. One of the two remaining fluorine atoms, F4, is terminal with a typical shorter  $\text{Ga}-\text{F}$  distance of 1.88  $\text{\AA}$ . Such a distance was previously observed in other gallium phosphates with a similar surrounding. For

(31) Kresge, C. T.; Leonowicz, M. E.; Roth, W. J.; Vartuli, J. C.; Beck, J. S. *Nature* **1992**, *359*, 710.

(32) Beck, J. S.; Vartuli, J. C.; Roth, W. J.; Leonowicz, M. E.; Kresge, C. T.; Schmitt, K. D.; Chu, C. T.-W.; Olson, D. H.; Sheppard, E. W.; McCullen, S. B.; Higgins, J. B.; Schlenker, J. L. *J. Am. Chem. Soc.* **1992**, *114*, 10834.

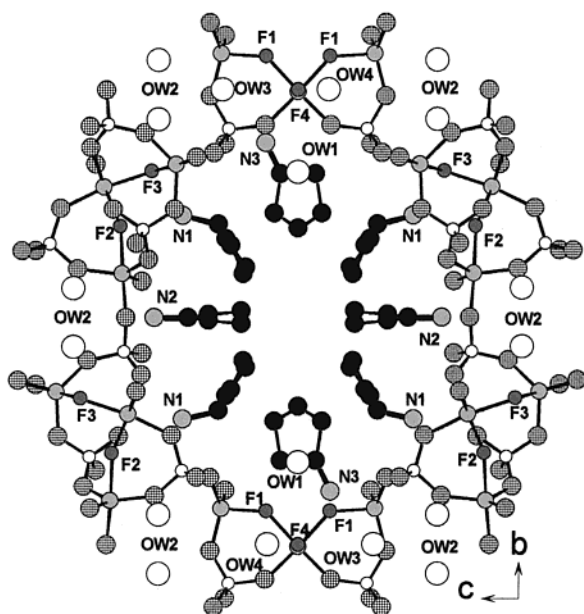


**Figure 5.** Configurations of the encapsulated cyclopentylamine and water molecules within the 18-ring tunnel: large open circles, water molecules; gray circles, nitrogen; dark gray circles, fluorine. The unlabeled atoms are as follows: black circles, carbon; hatched circles, oxygen; open circles, phosphorus; gray circles, gallium.

example, the terminal Ga–F bonding was 1.903 Å in GaPO<sub>4</sub>-CJ2<sup>33</sup> or 1.900 Å in p-KTP.<sup>34</sup> The last fluorine atom, F5, is in bridging position between two octahedral gallium atoms belonging to two adjacent pentameric units. The two other gallium atoms (Ga5) are coordinated with three oxygen atoms (Ga5–O in the range of 1.796–1.812 Å) and one fluorine atom (Ga5–F1 = 1.877 Å). This results a distorted tetrahedral configuration with some O–Ga–O angles close to 120° (instead of 109° for a regular tetrahedron) because of the shift of the gallium Ga5 from the center of the tetrahedron GaO<sub>3</sub>F toward the GaO<sub>3</sub> triangular plane. A thorough examination of the gallium–anion interactions scheme shows that the water molecule Ow2 is weakly linked to the gallium Ga5 (Ga5–Ow2 = 2.68 Å) and induces the distortion of the tetrahedron. This interaction is significant to shift the position of the gallium atom and lengthen the Ga–F1 bonding (1.877 Å instead of ~1.80 Å for Ga–O). The geometry of this second building unit is quite close to the hexameric unit described above for MIL-46 and ULM-16. They both consist of a central octahedral gallium linked to two other gallium atoms (formation of a cis gallium trimer) and two phosphate groups. The main difference comes from the presence of an additional phosphate group linked to the three gallium polyhedra in the hexameric species. From the chemical point of view, the addition of another phosphate is prevented by the occurrence of four fluorine atoms bonded to the central gallium atom Ga4. The Ga–F–P condensation was not observed in the fluorinated phosphates family meaning that another phosphorus atom cannot be connected to that gallium atom. Only two Ga–O–P linkages are possible from the GaO<sub>2</sub>F<sub>4</sub>

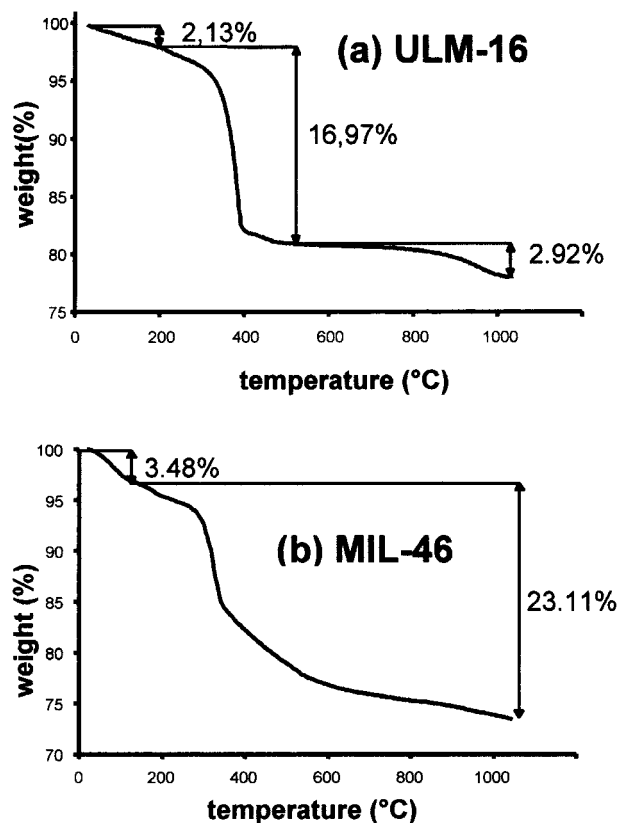


**Figure 6.** TGA curves of ULM-16 (a) and MIL-46 (b) under O<sub>2</sub> (2 °C/min).

unit. The higher fluorine concentration used in the hydrothermal reaction might be responsible for the formation of this rich fluorine building unit, which is unique in the fluorinated phosphates series. Along [100], two pentameric units are connected together via the Ga–O–P and Ga–F–Ga bondings and generate an isolated Ga<sub>6</sub>P<sub>4</sub> unit (Figure 4c) intercalated by water molecules and ammonium heads from the cyclopentylamine.

The three-dimensional network is built up from the corner sharing connection of these two types of units. Only the fluorine F4 is in terminal position. The resulting large 18-ring channels of approximately 10 Å × 13.1 Å in free diameter (based on an oxygen ionic radius of 1.35 Å) encapsulate the cyclopentylamine molecules and some water molecules. Other water molecules are also located within the six-ring channels. The three distinct cyclopentylamine molecules are protonated to balance the negative charges of the framework [Ga<sub>9</sub>(PO<sub>4</sub>)<sub>8</sub>F<sub>7.3</sub>(OH)<sub>0.2</sub>]<sup>4.5-</sup>. However, an excess of 0.5 negative charge is still present, and we assumed that 0.5 water molecule must be protonated as compensating positive charge. The ammonium groups interact with fluorine and oxygen atoms of the framework via hydrogen bond. Some short N···F and N···O distances are observed: N1···F2 = 2.85 Å; N1···F3 = 3.04 Å; N1···O4 = 2.99 Å; N1···O12 = 3.04 Å; N3···F4 = 2.84 Å. The interactions of the amine with the nitrogen atom N2 are slightly weaker and affect oxygen atoms only (N2···O5 = 3.10 Å, N2···O9 = 3.22 Å). The locations of the different cyclopentylamine molecules within the 16-ring pore are represented in the Figure 5. The orientation of the amine cycle is similar to that described in ULM-16: the ammonium heads interact with the inorganic

(33) Férey, G.; Loiseau, T.; Lacorre, P.; Taulelle, F. *J. Solid State Chem.* **1993**, *105*, 179.

(34) Loiseau, T.; Paulet, C.; Simon, N.; Munch, V.; Taulelle, F.; Férey, G. *Chem. Mater.* **2000**, *12*, 1393.



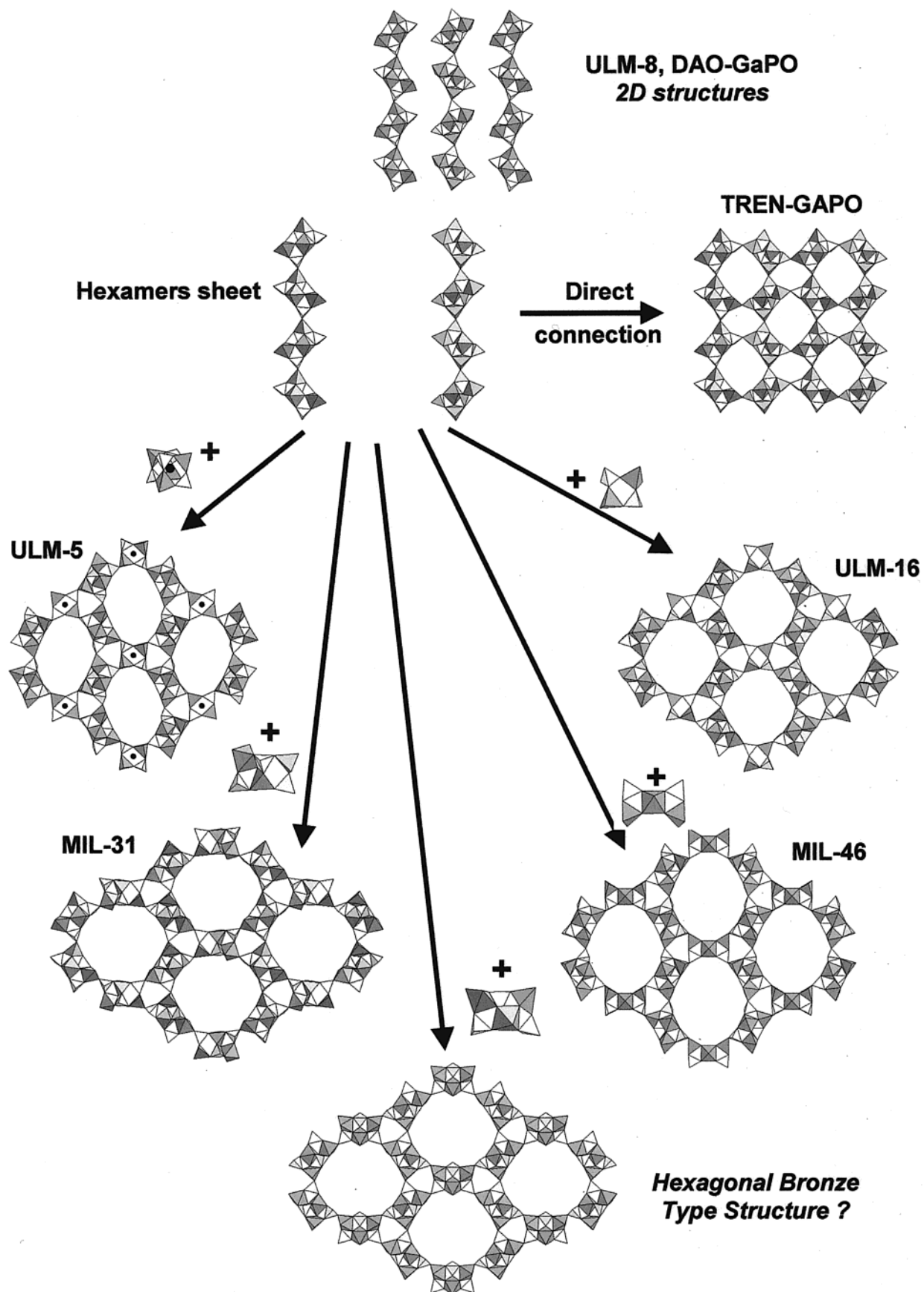


**Figure 7.** Occurrence of the layers of the hexameric building blocks  $\text{Ga}_3(\text{PO}_4)_3\text{F}_2$  in the fluorinated gallium phosphates. This specific hexamer sheet can be isolated in the two-dimensional compound ULM-8 or DAO-GaPO. The direct condensation of two sheets leads to the formation of TREN-GaPO. The addition of another building species between two hexamer sheets increases the pore size from 16-membered rings (ULM-5 and ULM-16) to 18-membered rings (MIL-31 and MIL-46). A hypothetical structure might be produced from the connection of the hexameric units only (hexagonal bronze structure-type).

walls of the cavities, and the cyclopentane part points toward the center of the channels. A surfactant-like behavior of this cyclic monoamine is also observed for the formation of the three-dimensional framework of MIL-46. Because of the size of the channels, two cyclopentylamines and two water molecules (for each  $\text{Ga}_{4.5}(\text{PO}_4)_4$  unit) are trapped within the pores of the MIL-46 framework. For comparison, the 16- and 6-ring channels observed in ULM-16 encapsulate 1.5 cyclopentylamines and one water molecule (for each  $\text{Ga}_4(\text{PO}_4)_4$  unit). The same configuration is encountered in the compound ULM-16 inserting the cyclohexylamine. For the last phase, the excess of one carbon atom on the cycle does not modify the resulting topology. An identical situation was observed for the ULM-3 topology prepared with three diamines with different alkyl chain lengths.<sup>35</sup> The compounds ULM-3 can be synthesized with 1,3-diamino-propane, -butane, and -pentane. These template species fit with the size and geometry of the 10-ring channels of ULM-3.

**Thermal Stability of ULM-16.** The TG curve of ULM-16 (Figure 6a) shows a three-step weight loss between 25 and 1050 °C. The initial weight loss below 250 °C may be due to the departure of water molecules (observed, 2.13%; expected, 2.13%). The second step occurring between 250 and 400 °C corresponds to the removal of the organic molecules together with  $1/3$  of the OH/F groups (observed, 16.97%; expected, 16.8%). The last event starting at 700 °C is assigned to the departure of the remaining F/OH groups (observed, 2.92%; expected, 2.9%). The XRD pattern of the residue at 1000 °C corresponds to the high cristobalite form of  $\text{GaPO}_4$ . The stability of the ULM-16 was also followed by thermodiffraction, which shows that the removal of the organic template affects the XRD pattern (400–700 °C). The identical low-angle Bragg peaks (at  $d \approx 14$  Å) are still observed, but other diffraction peaks disappear or appear indicating that another phase was formed. However, a detailed structural characterization of that compound was not possible because of the observation of a partial amorphization when the product is removed from the furnace and placed at ambient atmosphere. Then, this intermediate compound is transformed into dense  $\text{GaPO}_4$  from 700 °C. After dehydration, the ULM-16 compound rehydrates very slowly in air atmosphere.

**Thermal Stability of MIL-46.** The structure of MIL-46 is thermally less stable than ULM-16. The TG diagram (Figure 6b) indicates a two-step weight loss. The first event appears below 150 °C and is attributed to the loss of the occluded water molecules (observed, 3.48%; expected, 3.70%). The second loss (observed, 23.11%), which is continuous up to 1000 °C, is assigned to the removal of organic molecules (expected, 20.9%) and a part of the fluorine amount (expected, 7.3%). The XRD patterns show that the structure collapses from 200 °C and is amorphous up to 1050 °C. The thermal stability difference between ULM-16 and MIL-46 might be due to the fluorine content. The presence of a larger amount of fluorine in MIL-46, which allows for the formation of a more porous framework, would be a significant drawback for the thermal behavior.

## Discussion and Conclusion

The two fluorinated gallium phosphates ULM-16 and MIL-46 exhibit three-dimensional architectures delimiting large one-dimensional channels. The examination of their topologies shows a structural common part consisting of layers of hexameric blocks,  $\text{Ga}_3(\text{PO}_4)_3\text{F}_2$ , connected together via an additional building unit (Figure 7). The size of the latter will determine the space between the hexamer layers. For example, the direct condensation of such hexamer sheets was already described in the solid TREN-GAPO,<sup>15</sup> characterized by 12-ring channels. The ULM-16 framework involves the cyclic four-ring unit  $\text{Ga}_2\text{P}_2$  (generating an infinite double crankshaft chain) and a 16-ring channel is formed. Another 16-ring channels-based network is also reported for ULM-5<sup>18</sup> in which the cubic D4R unit plays the role of condensation between the hexamer layers. In MIL-46, the connection unit is a pentamer  $\text{Ga}_3\text{P}_2$ , which induces the formation of the 18-ring tunnels. Such a type of arrangement was previously described in the other 18-ring channel structure, MIL-31,<sup>20</sup> defined from the similar condensation of hexamer layers with a different geometry of building block (hexamer  $\text{Ga}_3\text{P}_3$ ). In this series of structures, the occurrence of the hexamer sheets is a constant and can be isolated as a layered-like arrangement in ULM-8<sup>27</sup> (inserting tris-(2-aminoethyl)amine molecule) or DAO-GaPO<sup>28</sup> (inserting 1,8-diaminooctane and pyridine). Because of its occurrence in several phases in the fluorinated GaPO series, this type of layered species was assumed to play a central role as intermediate phase for the condensation mechanisms during the hydrothermal treatment. The 3D solid would result from the condensation of the layered block with isolated species remaining in solution. However, the studies performed on the crystallization of ULM-5 by in situ X-ray diffraction<sup>36</sup> did not show any formation of such a bidimensional phase. For certain synthesis conditions, intermediate phases can be observed for very short times of reaction, and recent works in the ULM-3 system<sup>37</sup> indicated the formation of chainlike structures with  $\text{GaP}_2$  stoichiometry (tancoite chain) instead of a 2D structure with  $\text{Ga/P} = 1$ . The other point is that one may imagine other topologies based on the condensation of this hexamer layer by using the notion of scale chemistry developed by Férey.<sup>38</sup> For example, the framework obtained from the connection of hexamer sheets with the same type of hexameric unit was not produced yet. It would result in a hexagonal bronze structure, which has been described with octahedra as the primary building units in tungstate oxides<sup>39</sup> (HTB type). The arrangement of the building units ( $\text{MO}_6$  octahedron or  $\text{Ga}_3(\text{PO}_4)_3\text{F}_2$  hexamer) is identical, and only the size of the resulting pore would be different. One may also imagine the intercalation of larger species than hexamers between these layers of  $\text{Ga}_3(\text{PO}_4)_3\text{F}_2$ .

CM011247D

(36) Francis, R. J.; O'Brien, S.; Fogg, A. M.; Halasyamani, P. S.; O'Hare, D. *J. Am. Chem. Soc.* **1999**, *121*, 1002.

(37) Walton, R. I.; Millange, F.; O'Hare, D.; Paulet, C.; Loiseau, T.; Férey, G. *Chem. Mater.* **2000**, *12*, 4552.

(38) Férey, G. *J. Solid State Chem.* **2000**, *152*, 37.

(39) Magneli, A. *Acta Chem. Scand.* **1953**, *7*, 315.

(35) Loiseau, T.; Taulelle, F.; Férey, G. *Microporous Mater.* **1996**, *5*, 365.